Characteristics of high-performance steel fiber reinforced recycled aggregate concrete utilizing mineral filler

Osama Zaid [a,*], Faisal M. Mukhtar [b,c], Rebeca M-García [d],
Mohammad G. El Sherbiny [e], Abdeliazim M. Mohamed [f,g]

[a] Department of Structure Engineering, Military College of Engineering, Risalpur, National University of Sciences and Technology, Islamabad 44000, Pakistan
[b] Department of Civil and Environmental Engineering, King Fahd University of Petroleum and Minerals, Dhahran 31261, Saudi Arabia
[c] Interdisciplinary Research Center for Construction and Building Materials, King Fahd University of Petroleum and Minerals, Dhahran 31261, Saudi Arabia
[d] Department of Mining Technology, Topography and Structures, University of León. Campus de Vegazana s/n, 24071 León, Spain
[e] Structural Engineering and Construction Management, Faculty of Engineering, Future University in Egypt
[f] Prince Sattam Bin Abdulaziz University, College of engineering, Department of Civil Engineering, Al-Kharj 16273, Saudi Arabia
[g] Building and Construction Technology Department, Bayan College of Science and Technology, 210 Khartoum, Sudan

ARTICLE INFO

ABSTRACT

In current state of the World, the pollution is increasing very fast. One of its major reason is the production of huge quantity of cement which causes outflow of CO_2 into the environment and land dumping of construction and demolition waste which leads to the land pollution. In order to address this major issue, it is important to decrease the utilization of cement by substituting the cement with by product such as slag and using recycled aggregates as a replacement of natural aggregates. This research aimed to utilize evaluate the performance of sustainable high-performance concrete reinforced with steel fibers which is produced with recycled aggregate. Crushed stone aggregates are supplanted with recycled aggregates extracted from source concrete that had compression strength of 45 MPa and 85 MPa at proportions of 50% and 100%. Steel fibers are used at 2% to produce high-performance concrete, and in a few of the mixtures, the cement was substituted with granulated blast furnace slag. In addition to mechanical performance, the durability properties, i.e., electrical resistivity, drying shrinkage, and water absorption, of concrete blends were examined. The test outcomes show that high-performance concrete with the required characteristics can be developed utilizing recycled aggregates extracted from source concrete of high strength. The inclusion of double hooked end steel fibers considerably improves the mechanical characteristics of RAC. Concrete formed with high-quality recycled concrete aggregates and mixes comprising granulated blast furnace slag (GBFS) and double hooked end (DHE) steel fibers shows decreased drying shrinkage and water absorption in comparison to normal concrete. The outcomes of the present study assist in making of suitable high-performance concrete which is sustainable and budget friendly.

---

* Corresponding author.
E-mail address: osama.zaid@scetwah.edu.pk (O. Zaid).

1. Introduction

The volume of demolition and construction waste (CDW) is increasing significantly daily [1] worldwide. A considerable sum of this leftover is from structures of concrete that are demolished. It has been revealed that 0.32 billion to 0.40 billion tons of construction and demolition waste is being formed each year in European countries [2]. The substitution of normal weight aggregates with RCA not only decreases the necessity for using natural aggregates but also decreases the cost of transport and often emission [3]. Reusing and recycling discarded concrete is suitable and important from an eco-friendliness point of view and efficient consumption of natural resources [4–7]. Furthermore, the formation of RAC with the utilization of recycled concrete aggregate as a substitute for traditional concrete is essential because of the lack of natural aggregate (NA) stock in different portions of the earth [8]. Usually, the inferior performance of recycled concrete aggregate in comparison to natural aggregate often leads to concrete with poor mechanical, durability, and physical performance [9,10]. However, the utilization of an appropriate proportioning of materials [11,12] and the usage of mineral additives [12] may result in concrete with similar properties to NAC. The author in a study [13] revealed a new mixing technique (RAC) which also considers adhered cement paste on recycled concrete aggregate. Utilization of pozzolanic additives have amplified considerably in recent years due to awareness of environmental issues. Presently, the production of cement causes 8% of worldwide emissions of carbon dioxide (CO_2) yearly, and lowering this large outflow of CO_2 is a challenge worldwide [14]. The latest method to reduce this issue is to substitute cement with mineral additives. There are many mineral additives that are industrial byproducts or waste products that are utilized to decrease the content of cement needed and subsequently form more ecofriendly and sustainable concrete [15–17]. The most common mineral admixtures that are easily accessible are granulated blast furnace slag (GBFS), fly ash, and silica fume [18–20]. It is a well-known fact that granulated blast furnace slag (GBFS) is a useful additive for concrete and helps enhance the performance of concrete because of its pozzolanic impact [21,22]. Concrete mixed with GBFS can decrease the concrete porosity, alter the mineralogy of cement hydrates, and subsequently enhance the concrete durability performance [23,24].

The worldwide requirement for HPC has considerably amplified in the last decade [25,26]. High-performance concrete can be developed with high workability and improved mechanical and durability performance in comparison to conventional concrete [27, 28]. However, very limited research has been conducted on the inclusion of RCA and DHE steel fibers in high-performance concrete. It is a well-known fact that the quality of concrete made from extracted recycled aggregates has a significant impact on the performance of freshly mixed concrete [29,30]. It has been reported [31] that high-performance concrete could be effectively formed by utilizing recycled concrete coarse aggregates that were extracted from waste concrete, which had a compressive strength of more than 55 MPa. Regardless of the huge benefits of HPC, the high strength of high-performance concrete makes it susceptible to early cracking that may lead to serious degradation of the structure's life service [32]. Adding different types of fibers is known as a meaningful method of overcoming this drawback of HPC and developing concrete that has maximum flexural strength [33,34], tensile strength [35,36], ductility [37,38], and improved energy absorption capability due to less propagation of cracks [39].

1.1. Research significance

The present research aimed to examine the influence of recycled concrete aggregate that was extracted from waste concrete that had a compressive strength between 45 MPa and 85 MPa on the characteristics of high-performance concrete. The substitution of naturally occurring limestone coarse aggregate with RCA at substitution levels of 50% and 100%. Furthermore, the effect of substitution of the binder with 25% (GBFS) was also examined. Last, in only a few of the concrete blends, hooked end steel fibers were introduced at an amount of 2%. To the best of our knowledge, this is one of a few types of research on adding DHE steel fibers in high-
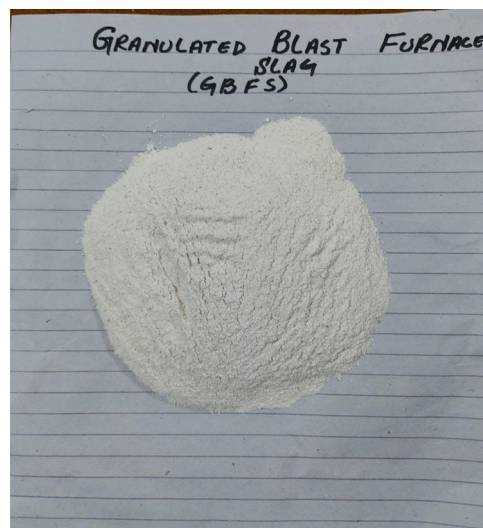

Fig. 1. Granulated Blast Furnace Slag (GBFS).

performance recycled aggregate concrete incorporating granulated blast furnace slag. Moreover, very little research is present on the durability performance, for example, electrical resistivity, drying shrinkage and water absorption of high-performance recycled aggregate concrete made with granulated blast furnace slag [40–42]. The flexural, split tensile, and compressive strength, electrical resistivity, water absorption, shrinkage of RAC were investigated. The results of the current study likely considerably increase the utilization of HPC produced with recycled concrete aggregate, slag and DHE steel fibers in various building applications.

2. Experimental plan

2.1. Materials

2.1.1. Cement and slag

Type I Portland cement per ASTM C150 was used as a primary binder in the present study. Granulated blast furnace slag as shown in Fig. 1 was procured from Pak steel Re Rolling mills. The specific surface areas of cement and GBFS were 295 and 469 m^2/kg, respectively. The chemical compositions evaluated by the X-ray diffraction (XRD) spectra of the granulated blast furnace slag are presented in Table 1 and Fig. 2, respectively. The X-ray diffraction (XRD) spectra of the GBFS, as displayed in Fig. 2, demonstrated an amorphous hump property at 38°, signifying the existence of a large content of alkaline calcium material. The chemical arrangement and physical characteristics of both GBFS and cement are presented in Table 1.

2.1.2. Aggregates

Crushed limestone was utilized as a natural coarse aggregate that had a maximum size of 25 mm and fineness modulus of 3.3. Coarse aggregates were used at 50% for both mixes. Two different kinds of aggregates were extracted from waste concrete: the first had a compressive strength of 45 MPa, and the other had a compressive strength of 85 MPa. The recycled coarse aggregates were acquired from concrete that was prepared in the lab utilizing similar natural aggregates as the reference samples, which were broken into pieces at a curing period of 56 days. The RCA was sieved after crushing to attain the same particle size distribution curve and maximum aggregate size as natural coarse aggregate. The physical characteristics of fine, recycled, and coarse aggregates are provided in Table 2. The density of natural aggregates was higher and the water absorption was lower than those of the recycled concrete aggregates. Furthermore, the physical characteristics of RCAs can be improved with the improvement in the strength of the source concrete. According to the author in the study [43], the method for processing RCAs also has a considerable effect on physical properties [43]. It was revealed that autogenous cleaning results in the development of RCA characteristics, mostly by plummeting the attached mortar on the surface of RCA; hence, water absorption was decreased. In the present research, the adhered mortar of recycled concrete aggregate was determined with the help of the dissolution of hydrochloric acid (HCl) process [44], and the test outcome is provided in Table 2. It was noted that the content of adhered mortar decreased with improving the strength of the source concrete.

2.1.3. Superplasticizer

To obtain the required workability and make the concrete sample workable and flowable, Viscocrete 3110 was used as an admixture in all blends.

2.1.4. Steel fibers

Double hooked end steel fibers that had a length of 55 mm and an aspect ratio of 62 are shown in Fig. 3. Its properties are presented in Table 3.

2.2. Mix proportioning

Entire samples of concrete had a cement amount of 550 kg/m^3, and the concrete was made with a constant water to cement ratio of 0.35. The complete mix proportions of all concrete samples are presented in a table. Four different groups of concrete mixes were developed, with each group comprising five different blends. High-performance concrete in group 1 was produced with different RCAs and in the absence of steel fibers and GBFS. In groups 2 and 4, cement was substituted by 25% GBFS, and the high-performance concrete in groups 3 and 4 comprised fixed 2% double hooked end steel fibers. Recycled concrete aggregate was included in the blends at percentage substitution of natural limestone coarse aggregate at rates of 50% and 100%. The recycled concrete aggregate was

Table 1
Chemical arrangement and Physical characteristics of slag and cement.

| Chemical configuration	Slag (%)	Cement (%)	Physical Characteristics	Cement	Physical Properties	Slag
CaO	40.2	62.9	Specific gravity (g/cm^3)	3.16	Specific gravity (g/cm^3)	3.45
Al2O3	10.4	5.5	Initial Setting time	125 min	Water absorption (%)	1.05
MgO	8.3	2.4	Final setting time	368 min	Bulk density (t/m^3)	1.96
SiO2	36.2	23.2	Compressive strength (MPa)		Fineness %	93
Fe2O3	1.8	2.9	3 days	21.4	Moisture content (%)	2.47
Na2O	1.5	0.5	7 days	28.5	Impact coefficient	9%
K2O	0.5	0.7	28 days	37.6	–	–
LOI	1.1	1.90	Soundness (%)	1.65	–	–
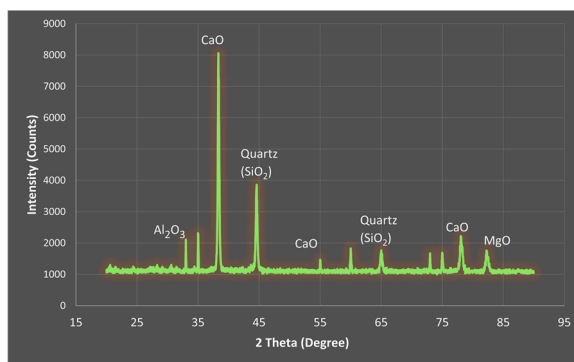
Fig. 2. XRD Pattern for Granulated Blast Furnace Slag (GBFS).

Table 2
Physical properties of fine and coarse aggregate.

Physical Property	Fine aggregate	Coarse aggregate	RCA (R85)	RCA (R45)
Maximum aggregate size (mm)	4.75	25	25	25
Adhered Mortar (%)	–	–	37	23
Flakiness Index (%)	–	13.4	13.92	14.21
Elongation Index (%)	–	13.85	14.1	14.4
Fineness Modulus	2.43	6.54	6.68	6.72
Bulk density (g/cm^3)	1.615	1.95	1.82	1.76
Water absorption (%)	0.94	0.65	2.53	2.86
Crushing value	–	16.95	21.84	23.89

Fig. 3. Double Hooked Steel Fibers.

Table 3
Properties of double Hooked end Steel Fibers.

Property	Value
Fiber Length (L)	55 mm
Diameter (d)	1.1 mm
Aspect ratio	62
Tensile Strength	2200 N/mm^2
Hook length	1–3 mm
Hook depth	1.70 mm

extracted from the 45 and 85 MPa compressive strengths because it was already available in the lab and is mentioned as R45 and R85. Fine and coarse aggregates were adopted in saturated surface dry conditions, whereas recycled concrete aggregate was used at the 75% saturation level. The admixture was added as a percentage of the total weight of cement. Complete mix details are provided in Table 4. To calculate the fresh concrete workability, a slump test was carried out following ASTM C143 [45] during the formation of concrete blends.

Table 4
Complete mix details of all concrete samples in kg/m^3.

Group	Mix ID	W/C	Water	Cement	GBFS	Aggregate				Steel Fibers	SP (%)	Slump (mm)
						Natural		Recycled				
						FA	NCA	R85	R45			
1	NAC	0.35	160	550	–	880	895	–	–	–	1.2	215
	R85–50	0.35	160	550	–	880	448	447	–	–	1.2	210
	R85–100	0.35	160	550	–	880	–	895	–	–	1.2	205
	R45–50	0.35	160	550	–	880	448	–	447	–	1.2	212
	R45–100	0.35	160	550	–	880	–	–	895	–	1.2	220
2	NAC-GBFS-25	0.35	160	412.5	137.5	880	915	–	–	–	1.2	195
	R85–50-GBFS-25	0.35	160	412.5	137.5	880	468	447	–	–	1.2	205
	R85–100-GBFS-25	0.35	160	412.5	137.5	880	–	915	–	–	1.2	200
	R45–50-GBFS-25	0.35	160	412.5	137.5	880	468	–	447	–	1.2	202
	R45–100-GBFS-25	0.35	160	412.5	137.5	880	–	–	915	–	1.2	210
3	NAC-S2	0.35	160	550	–	880	895	–	–	150	1.2	145
	R85–50-S2	0.35	160	550	–	880	448	447	–	150	1.2	140
	R85–100-S2	0.35	160	550	–	880	–	895	–	150	1.2	135
	R45–50-S2	0.35	160	550	–	880	448	–	447	150	1.2	140
	R45–100-S2	0.35	160	550	–	880	–	–	895	150	1.2	135
4	NAC-GBFS-25-S2	0.35	160	412.5	137.5	880	915	–	–	150	1.2	140
	R85–50-GBFS-25-S2	0.35	160	412.5	137.5	880	468	447	–	150	1.2	135
	R85–100-GBFS-25-S2	0.35	160	412.5	137.5	880	–	915	–	150	1.2	130
	R45–50-GBFS-25-S2	0.35	160	412.5	137.5	880	468	–	447	150	1.2	125
	R45–100-GBFS-25-S2	0.35	160	412.5	137.5	880	–	–	915	150	1.2	110

2.3. Sample molding and curing age

To determine the concrete compressive strength, 100 mm cubes were prepared following ASTM C 39 [46], and the samples were cured for 28, 56, and 90 days. For split tensile strength, 100 mm × 200 mm concrete cylinders were prepared and tested following ASTM C 496 [47] at a curing of 56 days. For concrete flexural strength, 150 mm × 150 mm x 600 mm concrete beams were prepared and tested following BS EN 14651 [48] at a curing period of 56 days. For electrical resistivity and water absorption tests of concrete, 100 mm concrete cubes were prepared per ASTM C 642 [49] and tested at curing ages of 28, 56, and 90 days. For the shrinkage test of concrete, ASTM C 157 [50] was followed, and 75 × 75×285 mm beams were prepared and tested in the lab at 56 days of curing. All the samples were removed from their molds after 24 h of casting and placed in water at a room temperature of 24 °C.

Fig. 4. Universal Testing Machine (UTM).

3. Testing procedure

3.1. Compressive, split tensile and flexural strength

Universal testing machine (UTM) as shown in Fig. 4 was utilized to estimate the mechanical strengths of concrete. The UTM had a capacity of 3000 KN. ASTM C 39 [46] and ASTM C 496 [47] were followed for compressive and split tensile strength, while BS EN 14651 [48] was followed for the determination of flexural strength.
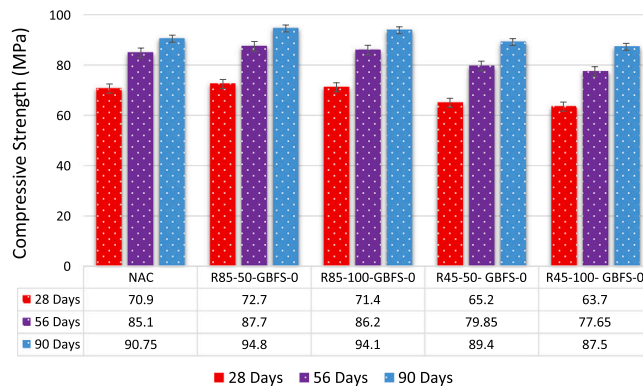
3.2. Water absorption

ASTM C642 [49] was followed to determine the concrete water absorption. This test was performed by calculating the difference in weight of the oven-dried sample and the sample that was cured in water for 28 days.

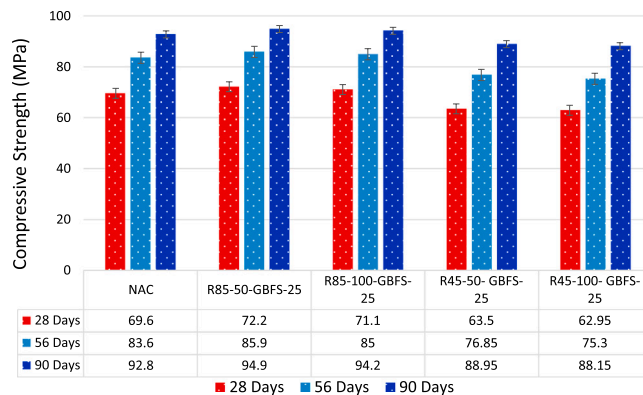### 3.3. Electrical resistivity

AC-impedance spectroscopy was utilized per ASTM C 1876 [51] to calculate the electrical resistivity of concrete, with a capacity of 2.0 MΩ and frequency of 1.5 kHz. All the samples were tested under SSD situations, and thin coat of binder mortar is provided amid copper plates and sample's surface to precisely determine the electrical resistivity.

3.4. Shrinkage

ASTM C 157 [50] was followed to perform this test on concrete prisms. The specimens for the shrinkage test were used in the moist condition in the molds for twenty-four hours enclosed with a cloth cover to shield samples from dipping water, and the samples were removed from the mold after that. When the samples were removed from the casts, the specimens were dipped in water for 45 min to reduce the change in length because of the temperature change. Afterward, the samples were pulled out from the water and cleaned with a fabric, and the primary comparator reading was calculated. Following ASTM C 157 [50], the specimens for the shrinkage test were placed in water

	NAC	R85-50-GBFS-0	R85-100-GBFS-0	R45-50- GBFS-0	R45-100- GBFS-0
28 Days	70.9	72.7	71.4	65.2	63.7
56 Days	85.1	87.7	86.2	79.85	77.65
90 Days	90.75	94.8	94.1	89.4	87.5

(a)

	NAC	R85-50-GBFS-25	R85-100-GBFS-25	R45-50- GBFS-25	R45-100- GBFS-25
28 Days	69.6	72.2	71.1	63.5	62.95
56 Days	83.6	85.9	85	76.85	75.3
90 Days	92.8	94.9	94.2	88.95	88.15

(b)

Fig. 5. Compressive strength of RAC at 28, 56 and 90 days (a) with 0% GBFS, (b) with 25% GBFS.

at 24 °C at a curing period of 56 days. It is well recognized that after 56 days, self-induced shrinkage is restricted, and more shrinkage is typically ascribed to self-dehydration [52,53]. The calculations for the shrinkage test were performed on samples at a room temperature of 24 °C and relative humidity of 45%.

4. Results and discussion

4.1. Compressive strength

The test outcome of compressive strength for all samples are presented in Figs. 5 and 6. It could be noted that the compressive strength of concrete samples created with 85 MPa recycled concrete aggregate is the same or somewhat greater than that of natural aggregate concrete samples at the same curing days. The substitution of NA with 45 MPa RAC led to a decrease in concrete compressive strength. The test outcome also showed that the compressive strength of concrete samples produced with 100% RAC was somewhat less than that of the concrete mix with 50% RCA. There are few aspects that influence the strength of RAC, including content of adhered paste, physical features of recycled concrete aggregate, and source concrete strength. The increase in the strength of 85 MPa recycled concrete aggregate blends with a 50% substitution level can be clarified by the added products of hydration caused by the attached mortar attached to RAC. The decrease observed in concrete strength with 100% recycled concrete aggregate can be ascribed to the weakness of recycled concrete aggregate in comparison to the natural aggregate, the effect of which develops further noteworthy in these blends because of the incremented amount. The test outcome showed that the compressive strengths of the R85–50 and R85–100 concrete samples were 5% and 2% greater than that of the natural aggregate sample, while the compressive strengths of the R45–50 and R45–100 blends were 7% and 11% lower than that of the natural aggregate concrete sample, respectively. Likewise, the higher strength of 85 MPa recycled aggregate concrete samples could be clarified by the fact that its source concrete strength was more than 45 MPa recycled aggregate concrete. The class of two ITZs amid the old and fresh paste and the old paste with the aggregate is a significant feature that considerably impacts the performance of RAC [54]. It is anticipated that the old interfacial transition zone amid the old mortar and the aggregate from RAC, especially in the situation of RAC extracted from sample with a lesser strength to be feebler compared to the new interfacial transition zone amid RAC and fresh mortar. Thus, the aged interfacial transition zone might be the primary surface where the crack comes. Subsequently, the R45–100 sample, due to the higher content of adhered mortar with an inferior class, displayed the lowermost compressive strength.
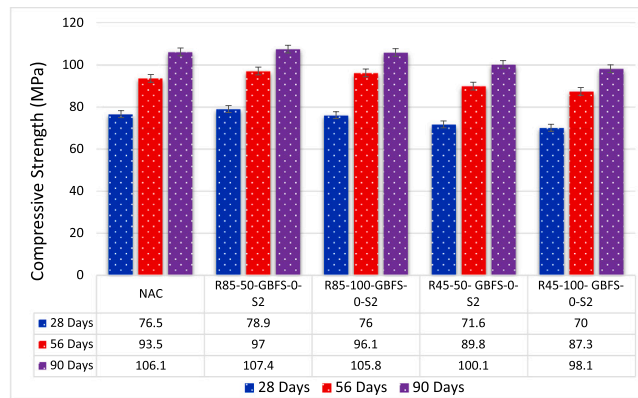
(a)
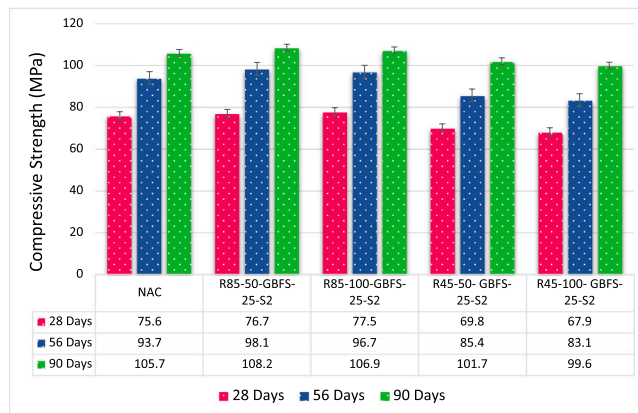
(b)

Fig. 6. Compressive strength of steel fiber-reinforced RAC at 28, 56 and 90 days (a) with 0% GBFS, (b) with 25% GBFS.

4.1.1. Compressive strength of concrete after addition of GBFS

As shown in Fig. 5, the replacement of Portland cement with 25% GBFS by cement weight results in a small decrease in concrete compressive strength at 28 and 56 days of curing. However, in the sample comprising GBFS, their compressive strength was identical or slightly greater than that of NAC at a curing period of 90 days. Adding GBFS can lead to enhancement in the adherence of the binder matrix, which decreases the initiation of microcracks, which leads to improvement in concrete strength [55]. Furthermore, GBFS fills the binder matrix capillary pores and subsequently enhances the performance of the ITZ [54]. In a study performed by the author [56], the X-ray diffraction (XRD) pattern of a 90-day hydrated specimen of Portland cement blend mixed with GBFS showed maximum reactivity of GBFS at this period in comparison to the early testing period. Hence, a minor decrease in early period strength was noted in the current research and could be ascribed to the lower rate of hydration of concrete comprising GBFS, which is very well recognized in the study [56,57]. The author in the study [58] revealed that replacing OPC with GBFS at a substitution rate lower than 55% may result in enhancement of both early and later curing days due to the maximum activation energy and proportion of calcium-silicate hydrate.

4.1.2. Compressive strength of concrete after addition of 2% double hooked steel fibers

Fig. 6 shows that adding 2% double hooked end steel fibers and 50% 85 MPa recycled aggregates to the concrete results in an improvement in the concrete compressive strength at all periods of curing. For example, the compressive strength of natural aggregate concrete comprising 2% steel fibers was enhanced by 8%, 11%, and 17% at 28, 56, and 90 curing days, respectively, in comparison to the concrete samples with no steel strands. Due to the more elastic modulus and specific shape of double hooked end steel fibers, it confines crack propagation, changes the crack tendency, and consequently enhances the concrete compressive strength [59]. The development in compressive strength of RAC comprising DHE steel strands ranged from 4% to 16% in comparison to natural aggregate concrete, relying on the grade and proportion of RCA. The compressive strength of RAC comprising GBFS and steel fibers was somewhat inferior at 28 and 56 days of curing than that samples with no GBFS, while their compressive strength at 90 days of curing was the same or slightly higher.

Mostly, the strongest growth rate in concrete mixes comprising RA, especially 45 MPa recycled concrete aggregate, was more than that in natural aggregate concrete. For example, the compressive strength of the natural aggregate concrete, R45-100, and R85-100 samples after curing for 90 days was 27%, 39%, and 32%, respectively, greater than 28 days of strength. This enhancement in strength can be clarified by the formation of more calcium-silicate-hydrate caused by the inside curing of the adhered mortar of recycled
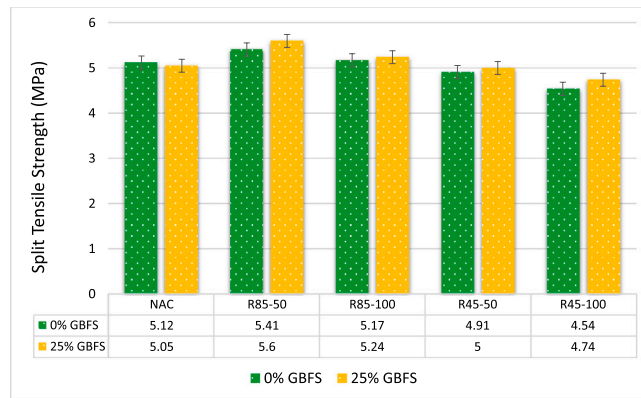
(a)
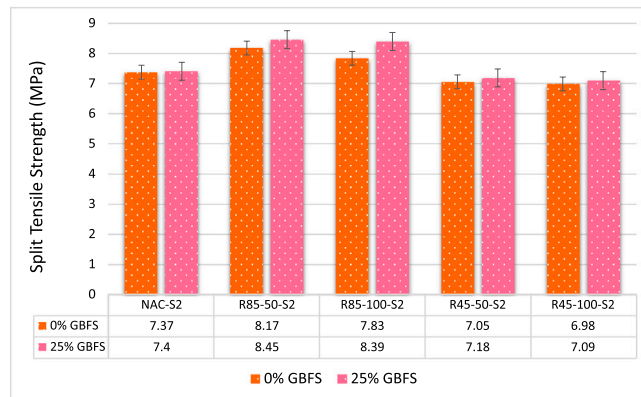
(b)

Fig. 7. Split tensile strength of recycled aggregate concrete at 56 days (a) with 0% steel fibers and (b) with 2% steel fibers.

concrete aggregate, which has been exhibited to lead to improvement in concrete microstructure [60,61]. Our test results showed a similar pattern of findings with past studies that depicted that RAC shows more strength gain at an extended curing period than normal concrete because of the enhanced interfacial transition zone and densifying binder matrix [62,63].

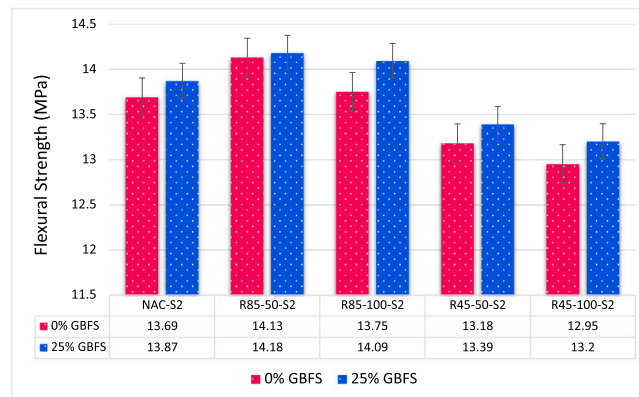### 4.2. Split tensile and flexural strength

The test outcomes of tensile and flexural strength for 56 days are presented in Figs. 7 and 8. The outcome of lab testing depicts that the inclusion of 85 MPa recycled concrete aggregate into concrete results in an improvement in both the flexural and splitting tensile strength of specimens. For example, the concrete split tensile strength comprising 50% and 100% 85 MPa recycled concrete aggregate was enhanced by 7% and 2%, respectively, in comparison to NAC. Instead, the concrete split tensile strength comprising 50% and 100% of 45 MPa recycled concrete aggregate was 5% and 12% lower than NAC, respectively. The enhanced flexural and split tensile strength of 85 MPa recycled concrete aggregate mixtures could be clarified by the enhanced bonding strength at the ITZ level amid the new and old binder paste [64]. Moreover, the high quality of 85 MPa recycled concrete aggregates and their role in the development of resultant calcium-silicate-hydrate are other contributory aspects to the enhanced strength. The physical characteristics of recycled concrete aggregate, such as its rough surface, may enhance the microstructure of the ITZ and consequently improve the concrete flexural and split tensile strength [65]. The decreased strength of concretes produced with 45 MPa recycled concrete aggregate could be ascribed to the enormous content of permeable mortar attached on the surface of RCA. The test outcome shows that an increment in the substitution level of recycled concrete aggregate from 50% to 100% results in a minor decrease in the strength.

4.2.1. Split tensile and flexural strength of concrete after addition of GBFS

The test outcome shows that the substitution of Portland cement with 25% GBFS had a very slight effect on the flexural and split tensile strength of NAC. However, a minor development in the strength of RCA was noted with the addition of GBFS. Fig. 7 shows that the split tensile strength of the mentioned mixtures was 9% and 4% greater than conventional sample. The enhanced performance might be clarified by capability of fine grain size of GBFS to enter the pores of RCA, improving the characteristics of the interfacial transition zone and bond between the binder matrix and aggregates [66].
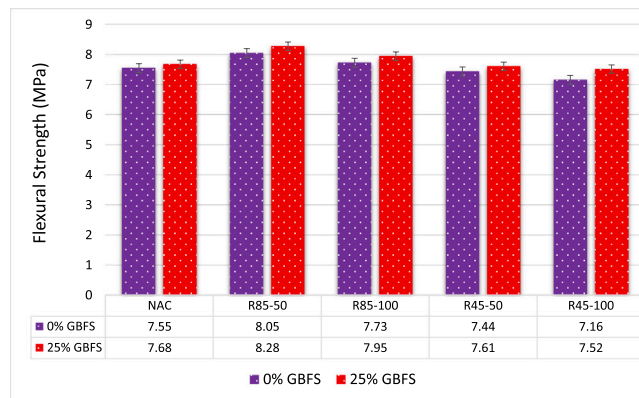
(a)

(b)

Fig. 8. Flexural strength of RAC at 56 days (a) with 0% steel fibers and (b) with 2% steel fibers.

4.2.2. Split tensile and flexural strength of concrete after addition of 2% double hooked steel fibers

The inclusion of 2% double hooked end steel fibers considerably improved the flexural and split tensile strength of all the mixtures. Figs. 7 and 8 show that the flexural and split tensile strengths of natural aggregate concrete comprising steel fibers were enhanced by 42% and 79%, respectively. Likewise, according to the author in the study [67,68], the introduction of DHE steel fibers at 1.5% or more results in considerable enhancement in both the post peak ductility and flexural strength of HSC. The test outcome also reveals that the DHE steel fibers were very active in enhancing the strength of RCA. For instance, the enhancement in split tensile strength of RCAs comprising steel fibers differs from 35% to 59%, whereas an 85% improvement in concrete flexural strength was obtained, relying on the type and number of RCAs. The enhancement is ascribed to the maximum tensile strength, effective anchoring mechanism, and high elastic modulus of double hooked end steel strands, due to which the propagation of microcracks was controlled in the concrete. The author in the study [69] revealed an improvement of up to 35% and 24% in the flexural and split tensile strength of RAC strengthened with 1% DHE steel fibers. The DHE steel fibers utilized in the current research showed considerably developed maximum pull-out forces in comparison to conventional steel fibers [68]. Consequently, maximum enhancement in the flexural and split tensile strength of concrete blends was obtained in this research in comparison to past studies, and steel fibers were utilized in that study. As shown in Figs. 7 and 8, the existence of DHE steel strands led to a considerable enhancement in the split tensile strength of RCA in comparison to natural aggregate concrete. For example, the split tensile strength of mixtures R45–100-S2 and R85–100-S2 improved by 52% and 50%, respectively, over the mixes that had no fibers, while the addition of fibers in a natural aggregate concrete blend resulted in an improvement of up to 43%. This could be ascribed to the improved bond between the binder paste and RCA because of the rough surface of the recycled concrete aggregate and the intertwining impact amid the recycled concrete aggregate and the fibers [70]. The test outcome also shows that among the various mixes considered in this research, the optimal performing blend was R85–50-GBFS-25-S2, which attained flexural and split tensile strengths of 14.12 MPa and 8.39 MPa, respectively (in comparison to the 7.49 MPa and 5.12 MPa of the natural aggregate concrete blend). The reference sample was split into 2 pieces, while this was restricted in the specimen comprising 2% double hooked end steel strands, as seen in Fig. 9(a and b), in which Fig. 9(a) shows failure of sample with no fibers and Fig. 9(b) shows the steel strands controlled the spread of microcracks, and cracks appeared only on the exterior surface of the concrete.
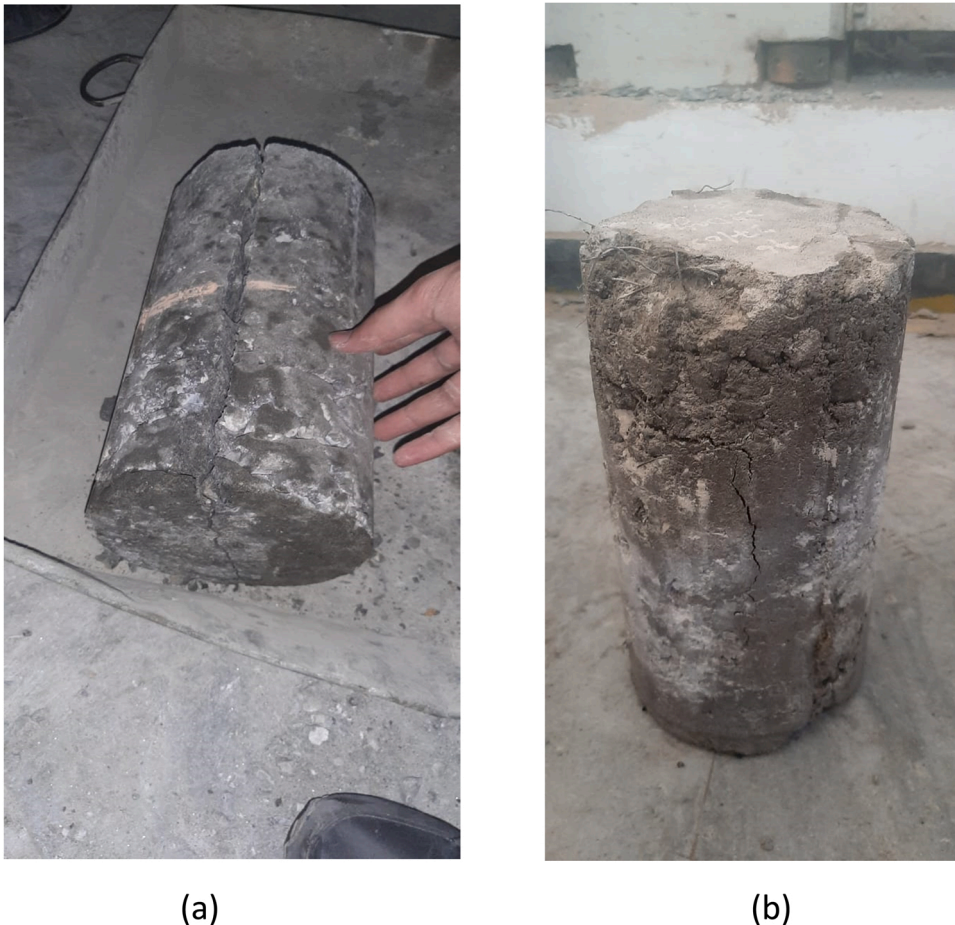

(a) (b)

Fig. 9. Failure of concrete sample under split tensile load (a) with no double hooked steel fibers, (b) with 2% double hooked steel fibers.

4.3. Water absorption

The test outcomes of the water absorption of RAC in the presence and absence of steel fibers and GBFS are presented in Fig. 10. As shown in Fig. 10, the substitution of natural aggregate with recycled concrete aggregate led to an increase in concrete water absorption. Fig. 10 also shows that there is a firm correlation between the content of recycled concrete aggregate and strength and the water absorption of the source concrete. For example, the substitution of 100% natural aggregate with 45 MPa and 85 MPa recycled concrete aggregate led to increase in water absorption by 56% and 25%, respectively. This could be ascribed to the large porosity of recycled concrete aggregate that initiates from the adhered mortar, and this was maximum for 45 MPa recycled concrete aggregates compared to 85 MPa recycled concrete aggregates. Increase in water absorption of up to 13.9% [71], 16.96% [72], 63% [73], and 69.25% [74] was noted in past studies with a complete change in coarse aggregates with RCAs.

4.3.1. Water absorption of concrete after addition of GBFS

The test outcome of water absorption also depicts that the addition of GBFS led to a decrease in water absorption. As shown in Fig. 10, the water absorption of natural aggregate concrete with GBFS was 13% less than that of the mix with no GBFS. A decrease of 16% was also noted in the water absorption of the R85–50-GBFS-25 mixture in comparison to the concrete mixture with no GBFS. This decrease could be ascribed to the capability of GBFS to develop the binder matrix at the microlevel by reducing the permeability and restricting the micro-openings connecting with each other [19]. Other than the pozzolanic behavior of GBFS, its filler impact may also have played a role in decreasing the water absorption due to the tiny particle size of GBFS. Because of this, GBFS may have entered the pores of recycled concrete aggregate and filled the cracks that initially existed in the recycled concrete aggregate with the product of hydration, consequently decreasing the concrete water absorption [41].

4.3.2. Water absorption of concrete after addition of 2% double hooked steel fibers

The test outcome of RCA strengthened with DHE steel strands showed that the addition of steel strands had a considerable impact on concrete water absorption. It could be noted that the water absorption of natural aggregate concrete decreased by 31% by adding 2% steel strands. Similarly, the water absorption of RCA comprising steel fibers was up to 22% less than that of the sample mixtures with no steel fibers. The test outcome proposes that the introduction of steel strands restrains the development and spreading of pores in the concrete, which leads to decreased permeability [75]. As noted in Fig. 10, the effect of DHE steel strands was more than GBFS on decreasing water captivation. The test outcome also shows that the lowest water absorption was obtained by the NAC-GBFS-25-S2 mixture, that displayed a 42% decrease in water captivation compared to the normal sample. Regardless of recycled concrete aggregate amount and sort, the water absorption of RAC comprising GBFS and DHE steel fibers are less than natural aggregate concrete. These explanations show that the inclusion of DHE steel strands and GBFS comprising recycled concrete aggregate can be developed to have comparatively less water absorption than natural aggregate concrete.

4.4. Electrical resistivity (ER)

The resistance to corrosion of concrete strengthening rebar can be examined by various methods. This test allows the assessment of risk to corrosion following existing standards [59]. It was suggested that electrical resistivity (ER) of more than 115 Ωm, between 60 and 115 Ωm and less than 60 Ωm can be utilized to signify the following likelihoods of corrosion of rebar: unlikely, likely, and unavoidable. The test outcome of the electrical resistivity of various RACs is presented in Fig. 11 (a, b and c) at 28, 56, and 90 curing days. The outcome shows that regardless of the type and amount of RA, the change in NA with recycled concrete aggregate results in a decrease in the concrete electrical resistivity (ER) at all curing days. Moreover, because of the high porosity and low quality of 45 MPa recycled concrete aggregate compared to 85 MPa recycled concrete aggregate, concrete comprising former aggregates displayed minimum electrical resistivity. Fig. 11 shows that an increase in the amount of recycled concrete aggregate instigated a decrease in the
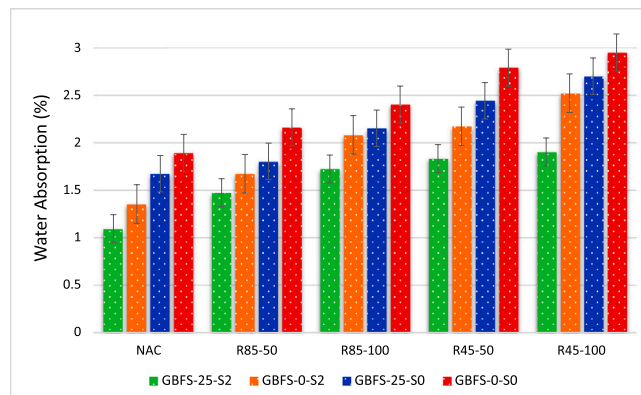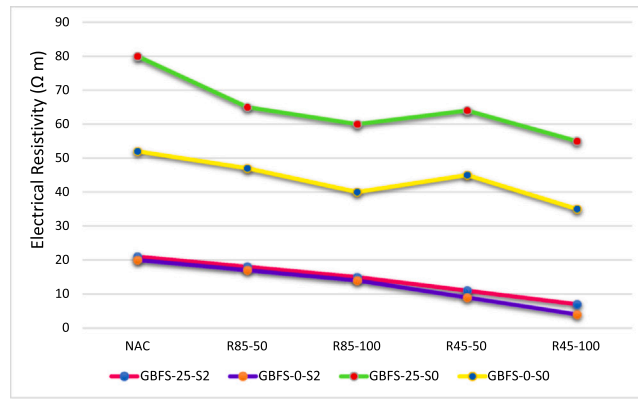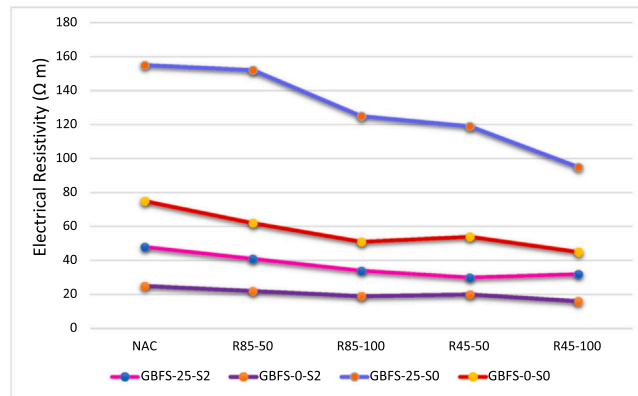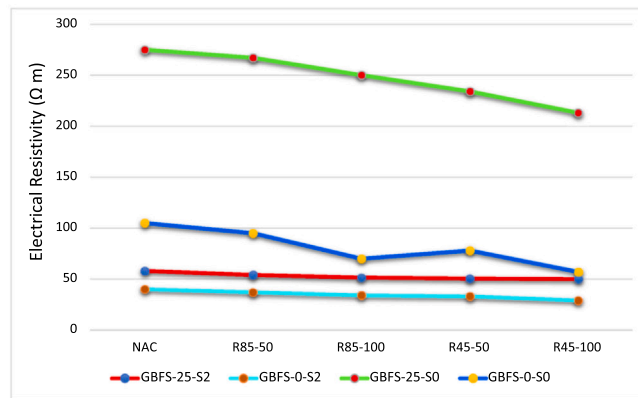

Fig. 10. Water absorption of RAC at 56 days.

(a)

(b)

(c)

Fig. 11. Electrical resistivity of RAC (a) at 28 days, (b) at 56 days, and (c) at 90 days.

ER. This could be clarified by the permeable behavior of RA that offers ions with a smooth condition to travel into concrete, which promotes the likelihood of rust of steel reinforcement [76]. Likewise, the maximum content of water inside the recycled concrete aggregate, caused by the perviousness, forms a situation that promotes chances of corrosion of steel reinforcement in sample [76]. The same results on the decrease in concrete electrical resistivity comprising recycled concrete aggregate were observed in past studies [76, 77]. As noted in Fig. 11, the decrease in RAC electrical resistivity ranged from 10% to 50%, reliant on the sort and amount and testing period of recycled concrete aggregate. The test outcome also shows that with the curing period, the RAC electrical resistivity is considerably enhanced in comparison to NAC. For example, the 90 curing days electrical resistivity of R45–50 and R85–50 mixtures were 140% and 149% more than curing of 28 days, respectively, while this enhancement was 127% for natural aggregate concrete mixtures. This could be ascribed to the formerly conferred effect of internal water curing and the development of extra calcium-silicate-hydrate that enhances the concrete microstructure and lowers the capillary pores [31].

*4.4.1. Electrical resistivity of concrete after addition of GBFS*

As noted in Fig. 11, the addition of GBFS to concrete considerably enhanced the concrete electrical resistance. The outcome shows that the addition of GBFS considerably enhanced the electrical resistivity, particularly at subsequent periods, such as 56 and 90 days. For example, the electrical resistivity of natural aggregate concrete containing GBFS was 55%, 114%, and 129% greater than that of the control sample at 28, 56, and 90 days, respectively. Because of the pozzolanic behavior of GBFS, it plays a role in the creation of secondary calcium-silicate-hydrate gel, which enhances the concrete microstructure and subsequently restricts the traveling of ions [78]. The gel of calcium-silicate hydrate, which is recognized as a basis of strength for sample, enhances solid phase volume and decreases the development of the capillary pore system in concrete. This process led to enhanced concrete durability performance, such as electrical resistivity [59]. The outcome of RAC containing GBFS shows that all of the specimens obtained maximum electrical resistance in comparison to the reference specimen. The enhancement in electrical resistivity ranged from 10% to 118%, reliant on the sort, amount, and testing period of recycled concrete aggregate.

4.4.2. Electrical resistivity of concrete after addition of 2% double hooked steel fibers

The outcomes of concrete with DHE steel fibers display a considerable fall in electrical resistivity. As observed from Fig. 11, steel fiber reinforced concrete obtained the minimum electrical resistivity amongst all the mixtures examined in this research. For example, the electrical resistivity of R45–100-S2 blends was 90%, 85%, and 83% lower than that of NAC at curing periods of 28, 56, and 90 days. This is because the conductivity of steel fibers significantly decreases the concrete electrical resistivity. From the classification in Fig. 9, the corrosion in concrete steel rebar formed in Groups 1, 2, and 3 would be likely unlikely and unavoidable after curing for 56 days. The utilization of steel fiber reinforced concrete in practical applications subjected to marine environments has been restricted because of steel fiber corrosion [79]. The author in the study [80] revealed the durability of SFRC by utilizing a quick migration assessment and noted a minor enhancement in the chloride diffusion of the mixture in comparison to the reference sample. The development of chloride ions at the interface of the steel strand and binder paste deteriorated the shielding oxide layer of the steel strands and consequently amplified the susceptibility to rust. Likewise, the author in the study [59] revealed that the addition of steel fibers resulted in a minor enhancement in chloride diffusion of FRC compared to normal concrete, which consequently led to a decrease in the usability of fiber-reinforced concrete structures. It was noted that lately established amorphous metal fibers have more resistance to corrosion [79] because of their specific composition, and they displayed no corrosion when submerged in hydrochloric acid (HCl) and sulfuric acid (H_2SO_4) for twenty-four hours.
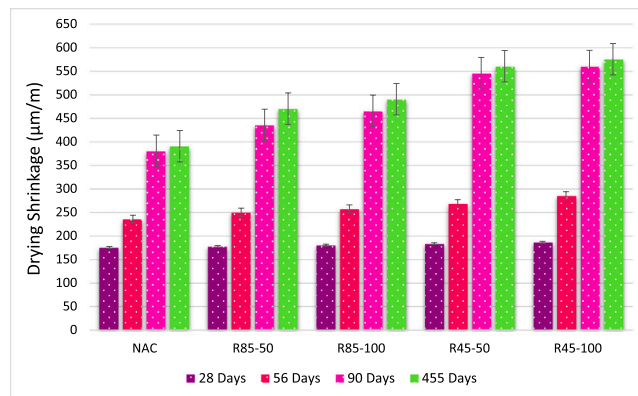
(a)
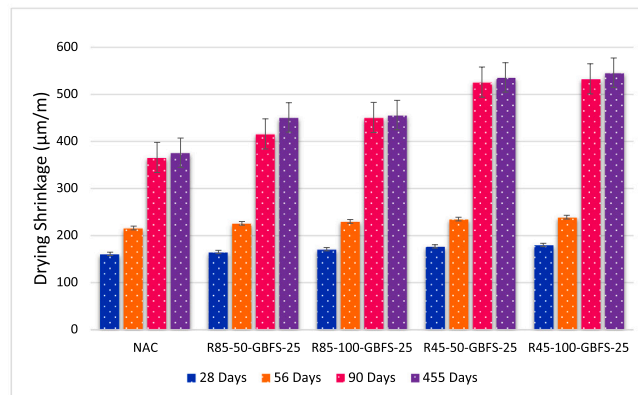
(b)

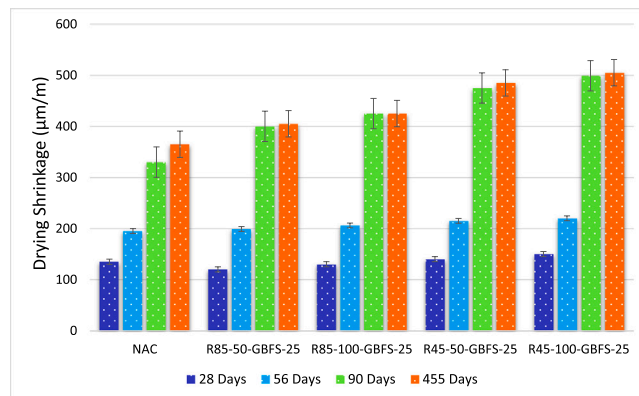**Fig. 12.** Drying shrinkage of RAC (a) with 0% GBFS, (b) with 25% GBFS.

4.5. Shrinkage test

The outcome of the shrinkage test performed under drying conditions is presented in Figs. 12 and 13. The relative shrinkage of RAC at curing periods of 28, 56, 90, and 455 days in comparison to the control natural aggregate concrete blend is presented in Fig. 14. The test outcome shows RA, regardless of the source concrete strength, displayed more shrinkage strain than the natural aggregate concrete blend. As noted in Fig. 12, the substitution of NA with RCA extracted from low strength source concrete and at more results in more shrinkage strains. The detrimental impact of recycled concrete aggregate on the concrete shrinkage was minimal when natural aggregate was substituted with 85 MPa recycled concrete aggregate. These test outcomes are similar to those of past studies on high-performance concrete comprising recycled concrete aggregate [81,82]. Likewise, the author in the study [83] revealed that the maximum shrinkage occurred in concrete incorporating the maximum substitution levels of RCA and poor quality of RCA. The concrete drying shrinkage strain is directly related to the content of free water kept in the capillary pores disperses because of the low humidity environment. This condition results in a humidity gradient that prompts the conveyance of particles of water from calcium-silicate-hydrate to the capillary pores afterward, which disperses [83]. The maximum content of unrestricted water in the capillary pores and permeability of RAC assists the conveyance of water and subsequently increases the drying shrinkage strain. As noted in Fig. 14, the shrinkage strain of RAC at 90 and 455 days was 19–67% and 18–46% greater than that of natural aggregate concrete, respectively, reliant on the substitution ratio and type of recycled concrete aggregate. These test outcomes show that the negative impact of RA on concrete shrinkage was somewhat alleviated by increasing the curing age of concrete.

4.5.1. Drying shrinkage of concrete after addition of GBFS

As noted in Fig. 14 (a), the substitution of Portland cement with 25% GBFS causes a decrease in the concrete shrinkage strain up to 12% in comparison to the control concrete at 90 days. This outcome is similar to the conclusions of past studies [84,85]. A similar pattern was also apparent in the RAC, and the samples containing GBFS formed a minor shrinkage strain in comparison to the samples with no GBFS. This decrease in the shrinkage strain could be clarified by the capability of GBFS to further increase the development of calcium-silicate-hydrate and ettringite at subsequent periods, subsequently resulting in a dense material with minimum porosity [86].

(a)
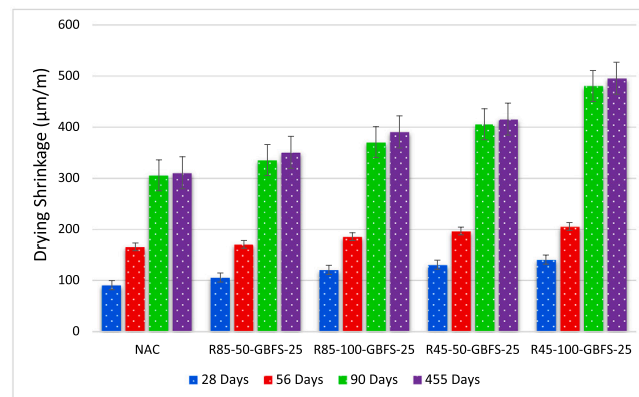
(b)

Fig. 13. Drying shrinkage of steel fiber reinforced RAC (a) with 0% GBFS, (b) with 25% GBFS.
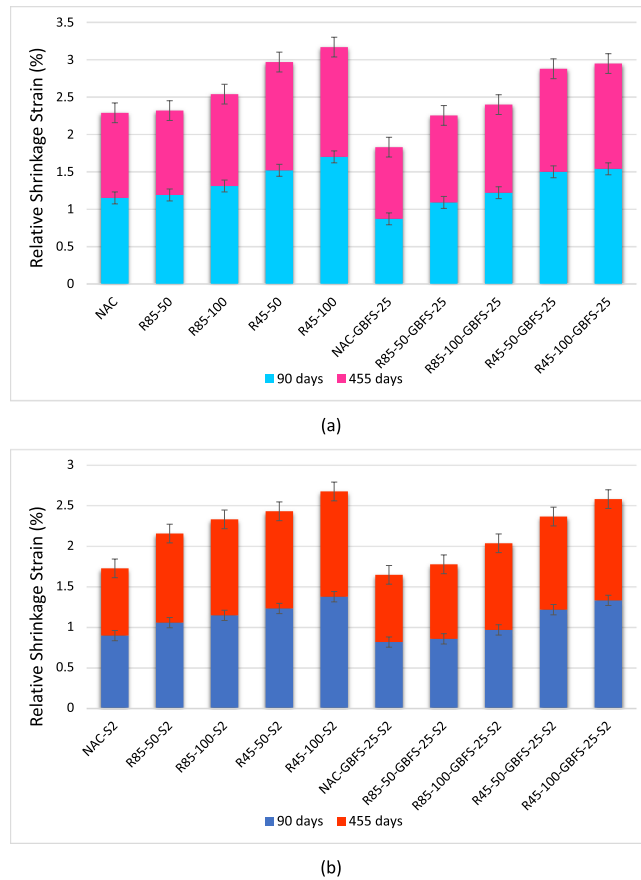
(a)

(b)

Fig. 14. Relative drying shrinkage of RAC (a) with 0% steel fibers and (b) with 2% steel fibers.

4.5.2. Drying shrinkage of concrete after addition of 2% double hooked steel fibers

The test outcome shows, introduction of steel strands results in decrease in shrinkage strain. The current outcome is between acceptable concurrence with past studies that demonstrated that steel strands can confine the spread of microcracks formed due to drying shrinkage [87,88]. As observed from Fig. 14 (b), steel strands were somewhat very significant in decreasing the drying shrinkage of RAC compared to natural aggregate concrete. For example, a decrease of 9% in 455 days shrinkage of natural aggregate concrete incorporating steel fibers was attained, whereas the decrease in the RAC comprising steel fibers was up to 16%. As observed from Fig. 14 (b), the minimalist shrinkage strain was attained by natural aggregate concrete comprising GBFS and DHE steel strands, while the highest strain was formed by the mixture incorporating 45 MPa recycled concrete aggregate at 100% substitution.

5. Life cycle analysis and sustainability performance

Concrete is one of the common materials that is used excessively in construction. Various researches are conducted in this field on various types of concrete for different resolves such as improving characteristics of concrete, life cycle, microstructure, sustainability. Presently researcher's [29] have performed their best to explore a way to use waste materials in the construction industry for the purpose of addressing the environmental issues. They have made considerable paces and on the base of their results [89], recycled aggregate concrete, by products (GBFS) for sustainable concrete could be consider as suitable option. Using GBFS as a partial substitute of cement will not help preserve the natural reserves of limestone but it will also assist in reducing the manufacturing of cement which will decrease the outflow of CO_2 into the atmosphere. Moreover, using recycled aggregates will also help in reserving the natural granite stone and also help the environment by reducing the land pollution caused from the construction and demolition waste.

6. Conclusions

This research studied the influence of granulated blast furnace slag and double hooked end steel fibers on the mechanical and durability performance of high-performance concrete incorporating RA of various grades and amounts. The following conclusions can be made from this study.

- Utilizing 85 MPa recycled concrete aggregate, high-performance concrete with similar mechanical performance to NAC can be developed. However, the usage of recycled concrete aggregate with low-quality source concrete decreases the concrete strength.
- Regardless of the kind and amount of RA, the usage of RCAs in high-performance concrete badly impacts the durability performance of concrete. Complete substitution of natural aggregate with 100% of 45 MPa recycled concrete aggregate led to 71% and 54% increase in the drying shrinkage and water absorption and a 51% reduction in concrete electrical resistivity.
- With the curing period, the electrical resistance of RAC varies considerably in comparison to normal concrete. Mixtures with 50% 45 MPa and 85 MPa recycled concrete aggregates sustained 141% and 149% increase in electrical resistivity at curing periods of 28 and 90 days, respectively.
- The addition of GBFS results in a decline in the concrete drying shrinkage and water absorption. The positive effect of GBFS becomes very distinct at a later period of curing.
- The influence of GBFS on the increase of RCA characteristics is comparatively higher than that of natural aggregate concrete. This could be clarified by the capability of fine GBFS particles to infiltrate inside the recycled aggregate pores, improving the characteristics of the interfacial transition zone and bond between the binder matrix and the aggregates.
- The introduction of DHE steel fibers to RAC at an amount of 2% resulted in an improvement of up to 65% in split tensile strength and 90% improvement in flexural strength at a curing period of 56 days.
- By insertion of DHE steel strands, electrical resistivity, shrinkage, and water absorption of natural aggregate concrete were reduced by 30%, 75%, and 11%, respectively, at a curing period of 56 days.

The outcome of this study showed that it is probable to produce eco-friendly high-performance concrete with durability and mechanical performance similar to natural aggregate concrete with the utilization of recycled concrete aggregate attained from high strength source concrete combined with GBFS and double hooked end steel fibers. These results are very promising and are directing to the likelihood of considerably decreasing any detrimental effect on the environment and developing high-performance concrete that has no compromise on strength and performance.

CRediT authorship contribution statement

Osama Zaid – Methodology, Writing, Conceptualization **Faisal Muhammad Mukhtar** - Methodology, Writing- review and editing **Rebeca Martínez-García** – Validation, Methodology **Mohammad Galal El Sherbiny** – Data Curation **Abdeliazim Mustafa Mohamed** - Validation

Declaration of Competing Interest

The authors declare that they have no known competing financial interests or personal relationships that could have appeared to influence the work reported in this paper.

Data availability statement

Data can be provided by demand from the corresponding author.

Acknowledgment

References

[1] O. Zaid, J. Ahmad, M.S. Siddique, et al., A step towards sustainable glass fiber reinforced concrete utilizing silica fume and waste coconut shell aggregate, Sci. Rep. 11 (2021) 1–14.
[2] J. Pacheco, J. de Brito, J. Ferreira, D. Soares, Dynamic characterization of full-scale structures made with recycled coarse aggregates, J. Clean. Prod. 142 (2017) 4195–4205, https://doi.org/10.1016/j.jclepro.2015.08.045.
[3] J. Ahmad, O. Zaid, C.L.-C. Pérez, et al., Experimental research on mechanical and permeability properties of nylon fiber reinforced recycled aggregate concrete with mineral admixture, Appl. Sci. 12 (2022), https://doi.org/10.3390/app12020554.
[4] S. Ghazizadeh, P. Duffour, N.T. Skipper, Y. Bai, Understanding the behaviour of graphene oxide in Portland cement paste, Cem. Concr. Res. 111 (2018) 169–182, https://doi.org/10.1016/j.cemconres.2018.05.016.
[5] İ.B. Topçu, S. Şengel, Properties of concretes produced with waste concrete aggregate, Cem. Concr. Res. 34 (2004) 1307–1312, https://doi.org/10.1016/j.cemconres.2003.12.019.
[6] A. Ajdukiewicz, A. Kliszczewicz, Influence of recycled aggregates on mechanical properties of HS/HPC, Cem. Concr. Compos 24 (2002) 269–279, https://doi.org/10.1016/S0958-9465(01)00012-9.
[7] P. Zhang, S. Han, S. Ng, X.-H. Wang, Fiber-reinforced concrete with application in civil engineering, Adv. Civ. Eng. 2018 (2018), 1698905, https://doi.org/10.1155/2018/1698905.
[8] R.V. Silva, J. de Brito, R.K. Dhir, Establishing a relationship between modulus of elasticity and compressive strength of recycled aggregate concrete, J. Clean. Prod. 112 (2016) 2171–2186, https://doi.org/10.1016/j.jclepro.2015.10.064.
[9] A.K. Padmini, R, K, M.S. Mathews, Influence of parent concrete on the properties of recycled aggregate concrete, Constr. Build. Mater. 23 (2009) 829–836, https://doi.org/10.1016/j.conbuildmat.2008.03.006.
[10] A. Corominas, M. Etxeberria, Effects of using recycled concrete aggregates on the shrinkage of high performance concrete, Constr. Build. Mater. 115 (2016) 32–41, https://doi.org/10.1016/j.conbuildmat.2016.04.031.

[11] G. Fathifazl, A. Abbas, G. Razaqpur, et al., New mixture proportioning method for concrete made with coarse recycled concrete aggregate. J Mater Civ Eng, J. Mater. Civ. Eng. (2009) 21, https://doi.org/10.1061/(ASCE)0899-1561(2009)21:10(601).

[12] H. Mefteh, O. Kebaili, H. Oucief, et al., Influence of moisture conditioning of recycled aggregates on the properties of fresh and hardened concrete, J. Clean. Prod. 54 (2013) 282–288, https://doi.org/10.1016/j.jclepro.2013.05.009.

[13] M. Pepe, R. Toledo Filho, E. Koenders, E. Martinelli, A novel mix design methodology for recycled aggregate concrete, Constuct. Build. Mater. 122 (2016) 362–372, https://doi.org/10.1016/j.conbuildmat.2016.06.061.

[14] K. Celik, M.D. Jackson, M. Mancio, et al., High-volume natural volcanic pozzolan and limestone powder as partial replacements for portland cement in self-compacting and sustainable concrete, Cem. Concr. Compos 45 (2014) 136–147, https://doi.org/10.1016/j.cemconcomp.2013.09.003.

[15] R. Yu, P. Spiesz, H.J.H. Brouwers, Development of an eco-friendly Ultra-High Performance Concrete (UHPC) with efficient cement and mineral admixtures uses, Cem. Concr. Compos 55 (2015) 383–394, https://doi.org/10.1016/j.cemconcomp.2014.09.024.

[16] H.T. Le, H.-M. Ludwig, Effect of rice husk ash and other mineral admixtures on properties of self-compacting high performance concrete, Mater. Des. 89 (2016) 156–166, https://doi.org/10.1016/j.matdes.2015.09.120.

[17] O. Zaid, J. Ahmad, M.S. Siddique, F. Aslam, Effect of incorporation of rice husk ash instead of cement on the performance of steel fibers reinforced concrete (https://doi:), Front Mater. 8 (2021) 14–28, https://doi.org/10.3389/fmats.2021.665625.

[18] P. Dinakar, K.P. Sethy, U.C. Sahoo, Design of self-compacting concrete with ground granulated blast furnace slag, Mater. Des. 43 (2013) 161–169, https://doi.org/10.1016/j.matdes.2012.06.049.

[19] S.C. Kou, C.S. Poon, M. Etxeberria, Residue strength, water absorption and pore size distributions of recycled aggregate concrete after exposure to elevated temperatures, Cem. Concr. Compos 53 (2014) 73–82, https://doi.org/10.1016/j.cemconcomp.2014.06.001.

[20] B. Joseph, G. Mathew, Influence of aggregate content on the behavior of fly ash based geopolymer concrete, Sci. Iran. 19 (2012) 1188–1194, https://doi.org/10.1016/j.scient.2012.07.006.

[21] H. Yazıcı, M.Y. Yardımcı, H. Yiğiter, et al., Mechanical properties of reactive powder concrete containing high volumes of ground granulated blast furnace slag, Cem. Concr. Compos 32 (2010) 639–648, https://doi.org/10.1016/j.cemconcomp.2010.07.005.

[22] S.E. Chidiac, D. Panesar, Evolution of mechanical properties of concrete containing ground granulated blast furnace slag and effects on the scaling resistance test at 28days, Cem. Concr. Compos 30 (2008) 63–71, https://doi.org/10.1016/j.cemconcomp.2007.09.003.

[23] H. Binici, H. Temiz, M.M. Köse, The effect of fineness on the properties of the blended cements incorporating ground granulated blast furnace slag and ground basaltic pumice, Constr. Build. Mater. 21 (2007) 1122–1128, https://doi.org/10.1016/j.conbuildmat.2005.11.005.

[24] A.E.B. Cabral, V. Schalch, D.C.C. Dal Molin, J.L.D. Ribeiro, Mechanical properties modeling of recycled aggregate concrete, Constr. Build. Mater. 24 (2010) 421–430.

[25] H.T. Le, M. Müller, K. Siewert, H.-M. Ludwig, The mix design for self-compacting high performance concrete containing various mineral admixtures, Mater. Des. 72 (2015) 51–62, https://doi.org/10.1016/j.matdes.2015.01.006.

[26] L. Biolzi, G.L. Guerrini, G. Rosati, Overall structural behavior of high strength concrete specimens, Constr. Build. Mater. 11 (1997) 57–63, https://doi.org/10.1016/S0950-0618(96)00026-8.

[27] I. Yurtdas, N. Burlion, J.-F. Shao, A. Li, Evolution of the mechanical behaviour of a high performance self-compacting concrete under drying, Cem. Concr. Compos 33 (2011) 380–388, https://doi.org/10.1016/j.cemconcomp.2010.12.002.

[28] A.H. Akca, N. Özyurt Zihnioğlu, High performance concrete under elevated temperatures, Constr. Build. Mater. 44 (2013) 317–328, https://doi.org/10.1016/j.conbuildmat.2013.03.005.

[29] S. Vaishnavi Devi, R. Gausikan, S. Chithambaranathan, J. Wilfred Jeffry, Utilization of recycled aggregate of construction and demolition waste as a sustainable material, Mater. Today Proc. 45 (2021) 6649–6654, https://doi.org/10.1016/j.matpr.2020.12.013.

[30] X. Liang, C. Wu, Y. Yang, Z. Li, Experimental study on ultra-high performance concrete with high fire resistance under simultaneous effect of elevated temperature and impact loading, Cem. Concr. Compos 98 (2019) 29–38, https://doi.org/10.1016/j.cemconcomp.2019.01.017.

[31] J. Ahmad Bhat, Effect of strength of parent concrete on the mechanical properties of recycled aggregate concrete, Mater. Today Proc. 42 (2021) 1462–1469, https://doi.org/10.1016/j.matpr.2021.01.310.

[32] A. Passuello, G. Moriconi, S.P. Shah, Cracking behavior of concrete with shrinkage reducing admixtures and PVA fibers, Cem. Concr. Compos 31 (2009) 699–704, https://doi.org/10.1016/j.cemconcomp.2009.08.004.

[33] L. Biolzi, S. Cattaneo, Response of steel fiber reinforced high strength concrete beams: experiments and code predictions, Cem. Concr. Compos 77 (2017) 1–13, https://doi.org/10.1016/j.cemconcomp.2016.12.002.

[34] S. He, E.-H. Yang, Non-normal distribution of residual flexural strengths of steel fiber reinforced concretes and its impacts on design and conformity assessment, Cem. Concr. Compos 123 (2021), 104207, https://doi.org/10.1016/j.cemconcomp.2021.104207.

[35] M. Nili, V. Afroughsabet, Combined effect of silica fume and steel fibers on the impact resistance and mechanical properties of concrete, Int J. Impact Eng. 37 (2010) 879–886, https://doi.org/10.1016/j.ijimpeng.2010.03.004.

[36] M.G. Alberti, A. Enfedaque, J.C. Gálvez, Fibre reinforced concrete with a combination of polyolefin and steel-hooked fibres, Compos Struct. 171 (2017) 317–325, https://doi.org/10.1016/j.compstruct.2017.03.033.

[37] M. Hasani, F. Moghadas Nejad, J. Sobhani, M. Chini, Mechanical and durability properties of fiber reinforced concrete overlay: Experimental results and numerical simulation, Constr. Build. Mater. 268 (2021), 121083, https://doi.org/10.1016/j.conbuildmat.2020.121083.

[38] K.G. Kuder, S.P. Shah, Processing of high-performance fiber-reinforced cement-based composites, Constr. Build. Mater. 24 (2010) 181–186, https://doi.org/10.1016/j.conbuildmat.2007.06.018.

[39] L. Biolzi, S. Cattaneo, G.L. Guerrini, Fracture of plain and fiber-reinforced high strength mortar slabs with EA and ESPI monitoring, Appl. Compos Mater. 7 (2000) 1–12, https://doi.org/10.1023/A:1008948125654.

[40] K.K. Sagoe-Crentsil, T. Brown, A.H. Taylor, Performance of concrete made with commercially produced coarse recycled concrete aggregate, Cem. Concr. Res. 31 (2001) 707–712, https://doi.org/10.1016/S0008-8846(00)00476-2.

[41] S. Kou, C. Poon, F. Agrela, Comparisons of natural and recycled aggregate concretes prepared with the addition of different mineral admixtures, Cem. Concr. Compos 33 (2011) 788–795, https://doi.org/10.1016/j.cemconcomp.2011.05.009.

[42] E. Anastasiou, K. Georgiadis Filikas, M. Stefanidou, Utilization of fine recycled aggregates in concrete with fly ash and steel slag, Constr. Build. Mater. 50 (2014) 154–161, https://doi.org/10.1016/j.conbuildmat.2013.09.037.

[43] M. Pepe, R.D. Toledo Filho, E.A.B. Koenders, E. Martinelli, Alternative processing procedures for recycled aggregates in structural concrete, Constr. Build. Mater. 69 (2014) 124–132, https://doi.org/10.1016/j.conbuildmat.2014.06.084.

[44] M. Ghalehnovi, A. Karimipour, A. Anvari, J. de Brito, Flexural strength enhancement of recycled aggregate concrete beams with steel fibre-reinforced concrete jacket, Eng. Struct. 240 (2021), 112325, https://doi.org/10.1016/j.engstruct.2021.112325.

[45] ASTM C 143 (2015) Standard Test Method for Slump of Hydraulic-Cement Concrete.

[46] ASTM C 39/C 39M-03 (2003) Standard Test Method for Compressive Strength of Cylindrical Concrete Specimens.

[47] ASTM C 496/-11 (2011) Standard Test Method for Splitting Tensile Strength of Cylindrical Concrete Specimens.

[48] BSEN 14651 (2007) Test method for metallic fibre concrete-measuring the flexural tensile strength (limit of proportionality (LOP), residual).

[49] ASTM C 642, Standard test method for specific gravity, absorption and voids in hardened concrete, Annual Book of ASTM Standards, West Conshohocken, 1997.

[50] ASTM C 157/C 157M-08 (2014) Standard test method for length change of hardened hydraulic-cement mortar and concrete.

[51] ASTM C1876 - 19 (2019) Standard Test Method for Electrical Resistivity or Conductivity of Concrete.

[52] Erika Holt (2001) Early age autogenous shrinkage of concrete: Dissertation.

[53] S. Boivin, P. Acker, S. Rigaud, B. Clavaud, Autogenous shrinkage of concrete, Autogen Shrinkage Concr. (1999) 81–92.

[54] L. Señas, C. Priano, S. Marfil, Influence of recycled aggregates on properties of self-consolidating concretes, Constr. Build. Mater. 113 (2016) 498–505, https://doi.org/10.1016/j.conbuildmat.2016.03.079.

[55] D.K. Panesar, J. Francis, Influence of limestone and slag on the pore structure of cement paste based on mercury intrusion porosimetry and water vapour sorption measurements, Constr. Build. Mater. 52 (2014) 52–58, https://doi.org/10.1016/j.conbuildmat.2013.11.022.

[56] R.L. Sharma, S.P. Pandey, Influence of mineral additives on the hydration characteristics of ordinary Portland cement, Cem. Concr. Res. 29 (1999) 1525–1529, https://doi.org/10.1016/S0008-8846(99)00104-0.

[57] J.S. Lumley, R.S. Gollop, G.K. Moir, H.F.W. Taylor, Degrees of reaction of the slag in some blends with Portland cements, Cem. Concr. Res 26 (1996) 139–151, https://doi.org/10.1016/0008-8846(95)00190-5.

[58] J.-M. Yang, D.-Y. Yoo, Y.-C. Kim, Y.-S. Yoon, Mechanical properties of steam cured high-strength steel fiber-reinforced concrete with high-volume blast furnace slag, Int J. Concr. Struct. Mater. 11 (2017) 391–401, https://doi.org/10.1007/s40069-017-0200-0.

[59] V. Afroughsabet, L. Biolzi, T. Ozbakkaloglu, High-performance fiber-reinforced concrete: a review, J. Mater. Sci. 51 (2016) 1–35, https://doi.org/10.1007/s10853-016-9917-4.

[60] M. Suzuki, M. Seddik Meddah, R. Sato, Use of porous ceramic waste aggregates for internal curing of high-performance concrete, Cem. Concr. Res 39 (2009) 373–381, https://doi.org/10.1016/j.cemconres.2009.01.007.

[61] V. Corinaldesi, Mechanical and elastic behaviour of concretes made of recycled-concrete coarse aggregates, Constr. Build. Mater. 24 (2010) 1616–1620, https://doi.org/10.1016/j.conbuildmat.2010.02.031.

[62] S.-C. Kou, C.-S. Poon, Long-term mechanical and durability properties of recycled aggregate concrete prepared with the incorporation of fly ash, Cem. Concr. Compos 37 (2013) 12–19, https://doi.org/10.1016/j.cemconcomp.2012.12.011.

[63] S. Zhutovsky, K. Kovler, Effect of internal curing on durability-related properties of high performance concrete, Cem. Concr. Res. 42 (2012) 20–26, https://doi.org/10.1016/j.cemconres.2011.07.012.

[64] W.-J. Long, D. Zheng, H. Duan, et al., Performance enhancement and environmental impact of cement composites containing graphene oxide with recycled fine aggregates, J. Clean. Prod. 194 (2018) 193–202, https://doi.org/10.1016/j.jclepro.2018.05.108.

[65] Z. Duan, C. Poon, Properties of recycled aggregate concrete made with recycled aggregates with different amounts of old adhered mortars, Mater. Des. 58 (2014) 19–29.

[66] Ö. Çakır, Experimental analysis of properties of recycled coarse aggregate (RCA) concrete with mineral additives, Constr. Build. Mater. 68 (2014) 17–25, https://doi.org/10.1016/j.conbuildmat.2014.06.032.

[67] G. Chen, D. Gao, H. Zhu, et al., Effects of novel multiple hooked-end steel fibres on flexural tensile behaviour of notched concrete beams with various strength grades, Structures 33 (2021) 3644–3654, https://doi.org/10.1016/j.istruc.2021.06.016.

[68] I. Ferdosian, A. Camões, Mechanical performance and post-cracking behavior of self-compacting steel-fiber reinforced eco-efficient ultra-high performance concrete, Cem. Concr. Compos 121 (2021), 104050, https://doi.org/10.1016/j.cemconcomp.2021.104050.

[69] J.A. Carneiro, P.R.L. Lima, M.B. Leite, R.D. Toledo Filho, Compressive stress–strain behavior of steel fiber reinforced-recycled aggregate concrete, Cem. Concr. Compos 46 (2014) 65–72, https://doi.org/10.1016/j.cemconcomp.2013.11.006.

[70] S.W. Tabsh, A.S. Abdelfatah, Influence of recycled concrete aggregates on strength properties of concrete, Constr. Build. Mater. 23 (2009) 1163–1167, https://doi.org/10.1016/j.conbuildmat.2008.06.007.

[71] M. Malešev, V. Radonjanin, S. Marinković, Recycled concrete as aggregate for structural concrete production, Sustainability 2 (2010) 1204–1225, https://doi.org/10.3390/su2051204.

[72] D. Matias, J. Brito, A. Rosa, D. Pedro, Durability of concrete with recycled coarse aggregates: influence of superplasticizers, J. Mater. Civ. Eng. 26 (2014), 6014011, https://doi.org/10.1061/(ASCE)MT.1943-5533.0000961.

[73] J. Correia, J. Brito, A. Pereira, Effects on concrete durability of using recycled ceramic aggregates, Mater. Struct. Constr. 39 (2006) 169–177, https://doi.org/10.1617/s11527-005-9014-7.

[74] C. Alexandridou, G.N. Angelopoulos, F.A. Coutelieris, Mechanical and durability performance of concrete produced with recycled aggregates from Greek construction and demolition waste plants, J. Clean. Prod. 176 (2018) 745–757, https://doi.org/10.1016/j.jclepro.2017.12.081.

[75] M. Nili, V. Afroughsabet, Property assessment of steel–fibre reinforced concrete made with silica fume, Constr. Build. Mater. 28 (2012) 664–669, https://doi.org/10.1016/j.conbuildmat.2011.10.027.

[76] N. Singh, S.P. Singh, Carbonation and electrical resistance of self compacting concrete made with recycled concrete aggregates and metakaolin, Constr. Build. Mater. 121 (2016) 400–409, https://doi.org/10.1016/j.conbuildmat.2016.06.009.

[77] S. Lotfi, M. Eggimann, E. Wagner, et al., Performance of recycled aggregate concrete based on a new concrete recycling technology, Constr. Build. Mater. 95 (2015) 243–256, https://doi.org/10.1016/j.conbuildmat.2015.07.021.

[78] H.-W. Song, V. Saraswathy, Studies on the corrosion resistance of reinforced steel in concrete with ground granulated blast-furnace slag—An overview, J. Hazard Mater. 138 (2006) 226–233, https://doi.org/10.1016/j.jhazmat.2006.07.022.

[79] D.-Y. Yoo, N. Banthia, J.-M. Yang, Y.-S. Yoon, Mechanical properties of corrosion-free and sustainable amorphous metallic fiber reinforced concrete, Acids Mater. J. 113 (2016) 633–643, https://doi.org/10.14359/51689108.

[80] C. Frazão, A. Camões, J. Barros, D. Gonçalves, Durability of steel fiber reinforced self-compacting concrete, Constr. Build. Mater. 80 (2015) 155–166, https://doi.org/10.1016/j.conbuildmat.2015.01.061.

[81] S.T. Yildirim, C. Meyer, S. Herfellner, Effects of internal curing on the strength, drying shrinkage and freeze–thaw resistance of concrete containing recycled concrete aggregates, Constr. Build. Mater. 91 (2015) 288–296, https://doi.org/10.1016/j.conbuildmat.2015.05.045.

[82] S.C. Kou, C.S. Poon, Enhancing the durability properties of concrete prepared with coarse recycled aggregate, Constr. Build. Mater. 35 (2012) 69–76, https://doi.org/10.1016/j.conbuildmat.2012.02.032.

[83] A. Gonzalez-Corominas, M. Etxeberria, Effects of using recycled concrete aggregates on the shrinkage of high performance concrete, Constr. Build. Mater. 115 (2016) 32–41, https://doi.org/10.1016/j.conbuildmat.2016.04.031.

[84] E. Güneyisi, M. Gesoğlu, E. Özbay, Strength and drying shrinkage properties of self-compacting concretes incorporating multi-system blended mineral admixtures, Constr. Build. Mater. 24 (2010) 1878–1887, https://doi.org/10.1016/j.conbuildmat.2010.04.015.

[85] D. Hooton, K. Stanish, J. Prusinski, The Effect of Ground, Granulated Blast Furnace Slag (Slag Cement) on the Drying Shrinkage of Concrete-A Critical Review of the Literature, Am Concr Institute, ACI Spec Publ,, 2004.

[86] J. Li, Y. Yao, A study on creep and drying shrinkage of high performance concrete, Cem. Concr. Res. 31 (2001) 1203–1206, https://doi.org/10.1016/S0008-8846(01)00539-7.

[87] A. Kaikea, D. Achoura, F. Duplan, L. Rizzuti, Effect of mineral admixtures and steel fiber volume contents on the behavior of high performance fiber reinforced concrete, Mater. Des. 63 (2014) 493–499, https://doi.org/10.1016/j.matdes.2014.06.066.

[88] C. Bywalski, M. Kamiński, M. Maszczak, Ł. Balbus, Influence of steel fibres addition on mechanical and selected rheological properties of steel fibre high-strength reinforced concrete, Arch. Civ. Mech. Eng. 15 (2015) 742–750, https://doi.org/10.1016/j.acme.2014.05.013.

[89] O. Zaid, F. Aslam, H. Alabduljabbar, To evaluate the performance of waste marble powder and wheat straw ash in steel fiber reinforced concrete, Struct. Concr. n/a (2021) 19–38, https://doi.org/10.1002/suco.202100736.